

## PERMEABILITY OF TEXTILE REINFORCEMENTS: SIMULATION; INFLUENCE OF SHEAR, NESTING AND BOUNDARY CONDITIONS; VALIDATION

B. Verleye<sup>1</sup>, R. Croce<sup>2</sup>, M. Griebel<sup>3</sup>, M. Klitz<sup>4</sup>, S.V. Lomov<sup>3\*</sup>, G. Morren<sup>4</sup>, H. Sol<sup>4</sup>,  
I. Verpoest<sup>3</sup> and D. Roose<sup>1</sup>

<sup>1</sup> *K.U.Leuven, Dept. Computer Science, Belgium*

<sup>2</sup> *University Bonn, Institute for Numerical Simulation, Germany*

<sup>3</sup> *K.U.Leuven, Dept. of Metallurgy and Materials Engineering, Belgium,*  
*corresponding author: Stepan.Lomov@mtm.kuleuven.be*

<sup>4</sup> *Vrije Univ. Brussel, Dept. of Mechanics of Material and Construction, Belgium*

**SUMMARY:** A fast and accurate simulation tool for the permeability of textiles is presented, based on a finite difference discretisation of the Stokes equations. Results for single layer, multi layer and sheared models are discussed. The influence of intra-yarn flow and periodic respectively wall boundary conditions are considered. Simulated permeability values are compared with experimental data. For the creation of the textile model the WiseTex software is used, which implements a generalised description of internal structure of textile reinforcements on the unit cell level. A finite difference Navier-Stokes solver, NaSt3DGP, was developed at the Institute for Numerical Simulation at the University of Bonn. The flow solver employs a Chorin projection on a staggered grid for the solution of the Navier-Stokes. In the staggered grid approach, the pressure is discretised at the centre of the cells, while the velocities are discretised on the edges. This discretisation leads to a strong coupling between pressure and velocities, and therefore avoids the occurrence of unphysical oscillations in the pressure. The experimental validation is performed with a highly automated central injection rig PIERS.

**KEYWORDS:** Textile composite, Fabric/textiles, Permeability, Modelling

### INTRODUCTION

Theoretical formulas for the calculation of the permeability of porous media such as textiles have been presented by several authors (Table 1).

Table 1 Methods for prediction permeability of textiles

<i>Method</i>	<i>Reference</i>	<i>Comment</i>
Theoretical formulas	1, 2, 3	Inaccurate for realistic textiles
FE modelling	4, 5, 6	Cumbersome meshing
lattice Boltzmann modelling	7	No acceleration techniques available
Grid2D	8	No validation for different kinds of textile
Pore network model	9	No satisfactory validation
Random walk methods	10	No satisfactory validation

We present the results of a finite difference solver: it works on a regular grid but more acceleration techniques for the resulting partial differential system of equations are available than for the lattice Boltzmann method. For the creation of the textile model, we use the WiseTex software [11]. WiseTex implements a generalised description of

the internal structure of textile reinforcements on the unit cell level. The WiseTex models are input for our permeability predicting software FlowTex.

### MATHEMATICAL MODEL

The permeability tensor  $\mathbf{K}$  is a geometric characteristic related to the structural features of the textile at several length scales. For a porous medium, the permeability tensor is defined by Darcy's law

$$\langle \mathbf{u} \rangle = -Re \cdot \mathbf{K} \cdot \langle \nabla p \rangle$$

with  $u = u(x, y, z)$  the fluid velocity,  $Re$  the Reynolds number,  $p = p(x, y, z)$  the pressure and  $\langle \rangle$  denotes volume averaging. In case of a creeping, single-phase, isothermal, unidirectional saturated flow of a Newtonian fluid, the inter-yarn flow is described by the incompressible Navier-Stokes equations,

$$\begin{cases} \frac{\partial \mathbf{u}}{\partial t} + (\mathbf{u} \cdot \nabla) \mathbf{u} = -\nabla p + \frac{1}{Re} \Delta \mathbf{u} \\ \nabla \cdot \mathbf{u} = 0 \\ \mathbf{u}|_{\mathbf{n}} = 0 \quad \text{and} \quad \nabla p|_{\mathbf{n}} = 0 \quad \text{on } \gamma. \end{cases}$$

Here  $\gamma$  denotes the boundary of the fluid and solid region and  $\mathbf{n}$  the outward-pointing unit normal vector on  $\gamma$ . The first equation states the conservation of momentum, the second equation states the conservation of mass. For the Reynolds numbers we are dealing with, i.e.  $Re \leq 1$ , the nonlinear convection term can be neglected. Since we are only interested in the steady state solution, the time derivative can be omitted. This results in the incompressible, steady Stokes equations,

$$\begin{cases} \Delta \mathbf{u} - Re \cdot \nabla p = 0 \\ \nabla \cdot \mathbf{u} = 0. \end{cases}$$

To determine the permeability from (1), the solution of (2) or (3) must be computed. Homogenisation of the Stokes equations in a porous medium yields Darcy's law (1) on macro level and can be applied within the periodic domain of a textile. In [12] we show that solving these equations to simulate the fluid flow and then using Darcy's law to calculate the permeability, results in the same numerical value as using the definition of  $\mathbf{K}$  arising from homogenisation theory.

Intra-yarn flow depends on the local permeability tensor of the yarn  $\mathbf{K}_{yarn}$  (calculated using formulae [1,2,3]), and is described by the Brinkman equations [13]

$$\begin{cases} \Delta \mathbf{u} - Re \cdot \nabla p = \mathbf{K}_{yarn}^{-1} \cdot \mathbf{u} \\ \nabla \cdot \mathbf{u} = 0. \end{cases}$$

### NUMERICAL APPROACH

For flow simulations in the irregular geometry of a textile, we solve the Navier-Stokes equations (2) and the Stokes equations (3) numerically on a regular grid with a finite difference discretisation. To this end, the geometry of the yarns is first order approximated. An example of a textile geometry and its first order approximation is shown in Figure 1.

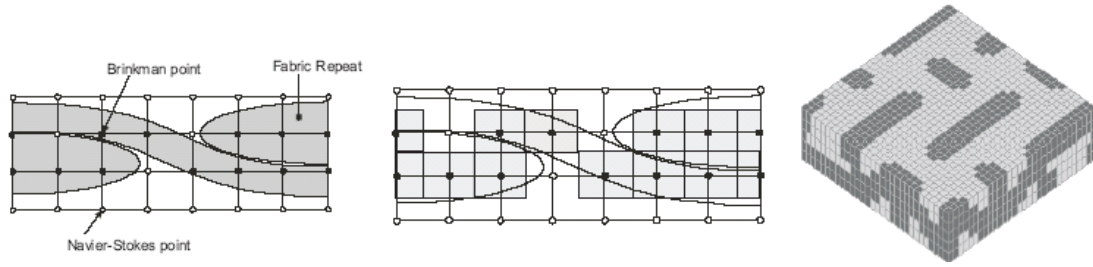


Figure 1 A 2D-textile model (left) and its first order approximation on the grid (middle); 3D voxel geometry (right)

## Boundary conditions

A boundary condition must be imposed between the yarn and fluid region. If we neglect the intra-yarn flow, the yarns are treated as impermeable. Each grid point is then either located in the fluid domain ('fluid points') or in the solid yarn domain ('solid points'). At the boundaries between the fluid and the solid, no-slip boundary conditions are imposed. We use a second order discretisation of the Navier-Stokes equations, but since the geometry is approximated to first order, we cannot expect second order accuracy near the boundaries. Including a second order description of the geometry would not only lead to the geometry modelling problems that we avoid by using the finite difference method, but a second order approximation of the boundary would also impose additional numerical stability problems. Although using a first order approximation of the yarns means that fine meshes are required to obtain an accurate result, it is shown in the validation section that we obtain permeability values within an acceptable computation time.

Boundary conditions must also be imposed on the boundary of the unit cell. In the XY direction it is obvious to use periodic boundary conditions because of the periodic structure of the textile. In the Z-direction however, both periodic and wall conditions can be justified: several layers of textile are put on top of each other in the mould, so periodic boundary conditions are acceptable. However, the mould is closed under pressure, and the thickness of the textile specimen may be too small to neglect the influence of the closed mould. Moreover, if several layers are put inside a mould, nesting of the layers is inevitable. If two layers nest, they form a closed layer between the other layers. In the validation section of this paper we show a comparison of the possible boundary conditions with experimental results.

## Solution of the Brinkman equations

The Brinkman equations use the same discretisation methods as the Navier-Stokes equations. They have to be solved in the yarn points if we take intra-yarn flow into account. We solve the Brinkman equations on the whole domain with  $||\mathbf{K}_{\text{tow}}|| = \infty$ , i.e. the Stokes equations, at fluid points while for yarns  $||\mathbf{K}_{\text{tow}}||$  is typically  $10^{-4} \leq ||\mathbf{K}_{\text{tow}}|| \leq 10^{-7}$ .

## Implementation

A finite difference Navier-Stokes solver, NaSt3DGP, was developed at the Institute for Numerical Simulation at the University of Bonn [14, 15]. The flow solver employs a Chorin projection method on a staggered grid for the solution of the Navier-Stokes equations. In the staggered grid approach, the pressure is discretised at the centre of the cells, while the velocities are discretised on the side surfaces. This discretisation leads to a strong coupling between pressure and velocities, and therefore avoids the occurrence of unphysical oscillations in the pressure. From a numerical point of view,

boundary conditions between the fluid and the solid region can be implemented in two ways:

- boundary values are set explicitly in the solid cells which are bordered by fluid cells;
- the boundary conditions are included in the equation to be solved in the boundary points in the fluid region.

NaSt3DGP sets the boundary values explicitly. On a staggered grid, this leads to the requirement that a solid point must be bordered by at least one other solid point in each direction. When the solid region forms very fine structures, as is the case for random fibre assemblies, e.g. non-wovens, this constraint leads to a very fine mesh (finer than required to capture the geometry itself and to obtain a sufficiently accurate solution).

The extension of NaSt3DGP towards a finite difference Stokes solver additionally uses the PETSc library [23] to solve the resulting system of discretised equations. Here, the discretisation has been realised on a collocated grid, i.e. all the unknowns are discretised in the centre of the cell, and includes the boundary conditions into the discrete system matrix.

## EXPERIMENTAL SETUP

The experimental prediction of the permeability on the majority of the textiles presented, is performed with a highly automated central injection rig, called PIERS set-up. This PIERS (Permeability Identification using Electrical Resistance Sensors) set-up consists of a mould cavity with two sensor plates, each containing 60 electrical sensors. After placing the reinforcement and closing the mould, the test fluid can be injected. This is done centrally in the reinforcement through a hole in the middle of the lower sensor plate. While the flow front propagates through the reinforcement, the fluid flow makes contact with the electrical sensors. Since an electrical conductive fluid is used, the wetting of these DC-resistance sensors will change their electrical resistance. This variation is registered and hence an arrival time for the sensors can be stored. From this data, the experimentally determined permeability is computed with an inverse method [16].

## VALIDATION

In this section our computations are validated against experimental results. Experimental verification of computational methods for the simulation of textile permeability is often missing in other papers on this subject. We demonstrate that our method is a general approach, valid for several types of textile structures. This is an important difference with other permeability predicting methods which rely on the structure of the textile. For example, special methods for the prediction of the permeability of non-crimp fabrics are presented in [17].

### Textile modelling

The methods and techniques to desing the used woven textiles and non crimp fabrics are explained in [11]. The multi-layered models, with or without nesting, are described in [18].

The geometrical description of internal structure of non-woven material is based on the following data:

- Fibre volume fraction of the material;
- Fibre geometrical (diameter, linear density) and mechanical properties;
- Distribution of the fibre length;
- Fibre orientation distribution, given as 2nd order orientation tensor;

- Fibre waviness. expressed as random combination of two harmonics.

The geometrical model uses these parameters of the individual fibres and creates a random fibrous assembly via a hierarchy of modelled objects:

- Straight fibre, characterised by fibre properties, length and orientation
- Curved fibre, modelled as consisting of several straight intervals, and characterised by fibre properties, total length, averaged orientation of the intervals and shape of the fibre, generated using the given waviness parameters
- Random realisation of an assembly of a given number of (curved or straight) fibres.

The boundaries of the unit cell of the material (where all the centres of gravity of the fibres are randomly placed) are calculated based on the given fibre volume fraction and thickness of the non-woven fabric. The given number of fibres is randomly generated by the model according to the given distributions of length, orientation and waviness of the fibres. In the case of non-woven fabric (as opposed to bulk material) the orientation is corrected to fit all the fibres inside the given thickness of the fabric. The random realisation of non-woven assembly is considered periodic; the degree of stochasticity included in the description is regulated by the number of the fibres in the assembly.

### Experimental validation

Figure 2 presents experimental and numerical results for two non crimp fabrics, a bi-axial and a quadri-axial. On the bi-axial structure, three institutes performed the experiments: MTM (K.U.Leuven), EPFL (Lausanne) and Ecole des Mines (Douai). The non crimp fabric has a dense structure which results in a high influence of the intra-yarn flow. For the quadriaxial non crimp fabric the computed permeability without Brinkman flow is  $5.3E-04$ , which is a large underestimation of the experimental permeability).

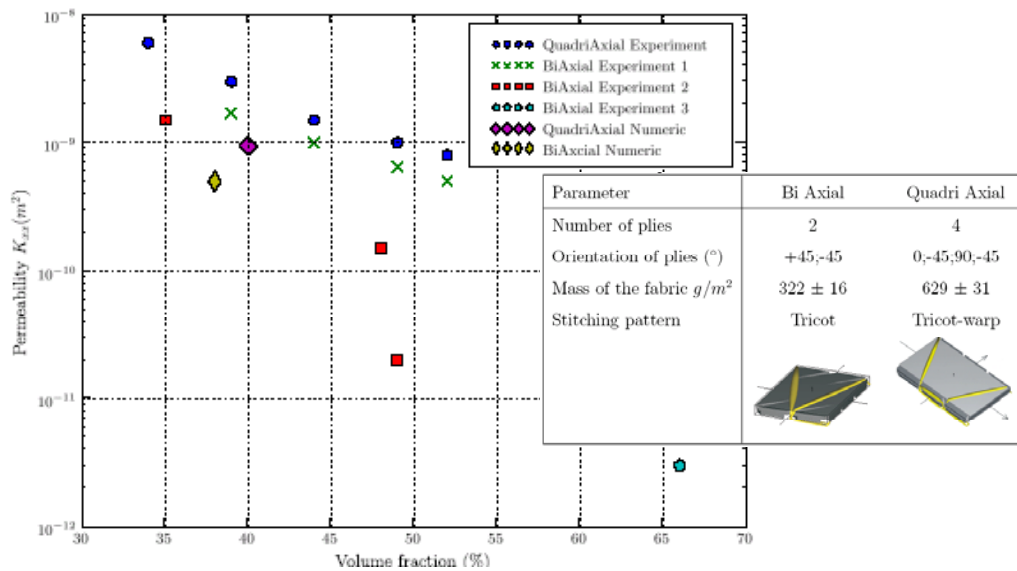


Figure 2 Experimental and numerical data of non crimp fabrics

For two woven fabrics Table 3 presents a picture of the textile model and the parameter details. The computed permeabilities of the MonoFilament Fabric (MFF) and the Plain Woven Fabric (PWF) are depicted in Figure 3. For both textiles two results with different volume fraction  $V_f$  are presented. For the low  $V_f$ , the computation was performed on a single layer model with wall boundary conditions. Although the experiments are performed on several layers, periodic boundary

conditions yield an overestimation of the permeability as the layers will nest and form a wall around the other layers. The high  $V_f$  result is obtained by modelling a three layered model with maximal nesting. Then, the middle part of the model, where the nesting actually occurs, is extruded, and wall conditions are imposed.

Table 2 Parameters of woven fabrics

Parameter	PWF	MFF	Random Mat
Width warp yarns (mm)	2.21	0.75	NA
Gap warp (mm)	0.58	0.44	NA
Width fill yarns (mm)	2.79	0.66	NA
Gap fill (mm)	0.35	0.34	NA
Areal density ( $\text{g}/\text{m}^2$ )	420	390	580
Specific density ( $\text{kg}/\text{m}^3$ )	2520	1423	2520
Yarn tex warp ( $\text{g}/\text{km}$ )	580	115	NA
Yarn tex weft ( $\text{g}/\text{km}$ )	600	115	NA

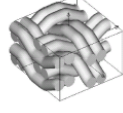
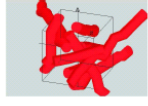




Figure 3 also presents the results for a non woven random mat. Unfortunately for this random structure no detailed information is available. However, given a certain  $V_f$  and a diameter of the fibres taken from an available picture, the geometry is approximated as good as possible, and the computed permeability values are close to the experimentally obtained values. The computed value is an average of computations on five random structures.

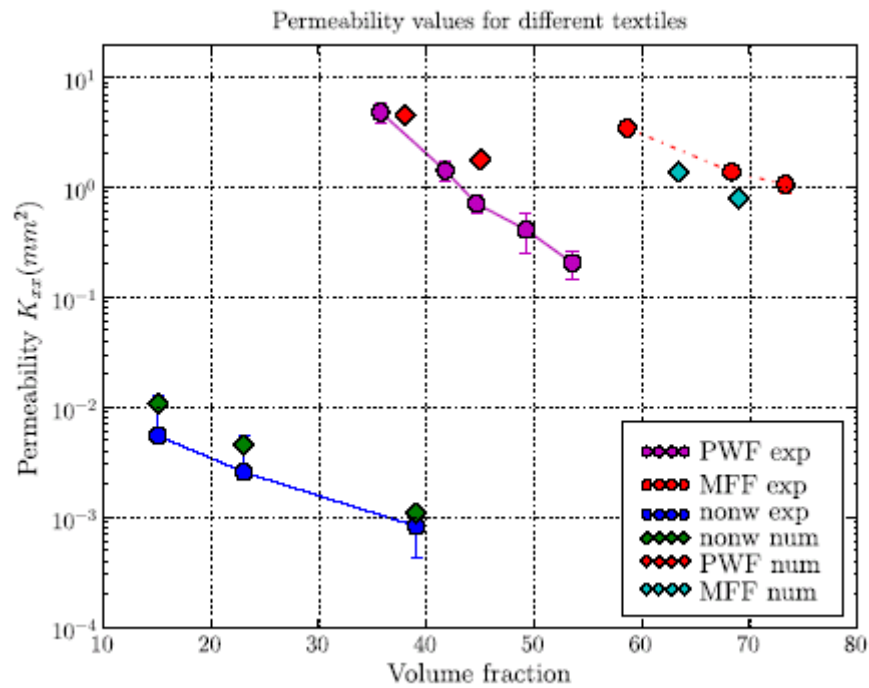


Figure 3 Experimental and numerical data of the PWF, MFF and the random mat

## Influence of shear

WiseTex allows the modelling of shear on the textile [19]. The sheared unit cell has however, no orthogonal repeat. This means that the periodic boundary conditions of the simulation software have to be put parallel to the direction of shear, and not, like in the original case, parallel to the orthogonal system axis. We have adapted our simulation software in order to compute the permeability in a sheared unit cell. To validate the results, we compare the computations with analytical formulas from Lai and Young [20] – Figure 4.

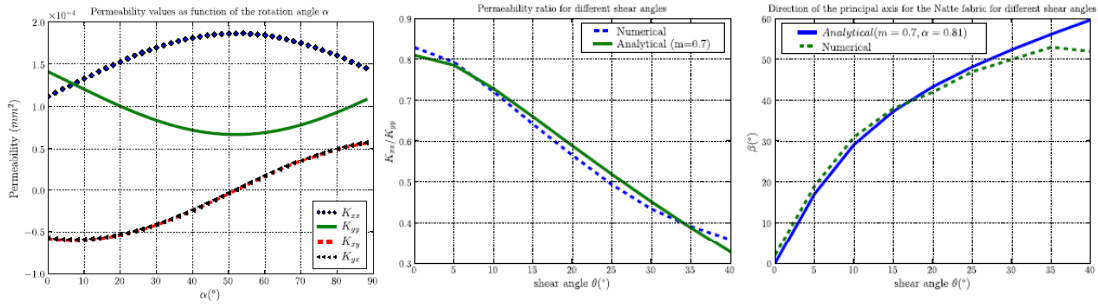


Figure 4 Sheared MMF fabric: (a) The components of the permeability tensor as function of the system rotation angle, (b) the direction of the principal axis as function of shear angle; (c) the anisotropy

## Computation time

The Navier-Stokes solver uses time stepping to reach the steady state solution in which we are interested. This time stepping procedure can be performed implicitly or explicitly. If implicit time stepping is used, the stability criterion is less restrictive and larger time steps can be taken which results in a faster solution (Table 4). The Stokes solver computes the steady state solution directly, and is substantially faster than the time stepping methods. For a fine grid,  $dx = 0.02\text{mm}$ , the solver only needs approximately one minute.

Table 3 Permeability values and computation time for a single layer model with XYZ periodic boundary conditions of the MFF

$\Delta x(\text{mm})$	$K_{xx}(\text{mm}^2)$	Comp. Time NaSt3D	Comp. Time Stokes
0.02	$3.3E - 04$	16 min 00 sec	00 min 46 sec
0.03	$3.4E - 04$	03 min 40 sec	00 min 26 sec
0.04	$4.3E - 04$	01 min 11 sec	00 min 05 sec

## CONCLUSIONS

In this paper a general approach for the computation of the permeability of textiles was presented. Solving the Stokes equations with a finite difference discretisation on a regular grid has the advantage that the solver can be used for any kind of textile structure without meshing problems. Although methods designed for specific textiles may lead to a faster solution, they only work for that specific structure and have to be redeveloped for new textiles. Moreover, fast and reliable solvers for PDE's are used in our permeability simulations.

For different textiles experimental validation was presented: for non crimp fabrics, woven fabrics and a random mat. Computations on a single layer model with periodic

boundary conditions result in a small over estimation of the experimental value, as nesting is neglected. Therefore multi layered models are to be used in the simulations, and wall conditions are to be imposed. For textiles with a high volume fraction, intra-yarn flow has an important influence on the permeability value. The micro flow is accounted for by solving the Brinkman equations. Not only nesting, boundary conditions and intra-yarn flow influence the permeability, also the shear of the specimen plays an important role. Our method is able to model shear and compute the permeability of the sheared models.

## REFERENCES

- 1 B. Gebart, Permeability of unidirectional reinforcements for rtm, *Journal of Composite Materials* 26 (8) (1992) 1100–33.
- 2 A. Berdichevski, Z. Cai, Preform permeability predictions by self-consistent method and finite element simulation, *Polymer Composites* 14 (2) (1993) 132–43.
- 3 F. Phelan, G. Wise, Analysis of transverse flow in aligned fibrous porous media, *Composites part A* 27A (1996) 25–34.
- 4 B. Laine, G. Hivet, P. Boisse, F. Boust, S. Lomov, P. Badel, Permeability of the woven fabrics, in: C. Binetruy (Ed.), *Proceedings of the 8th international conference on flow processes in composite materials*, Ecole des Mines de Douai, France, 2006, pp. 39–46.
- 5 N. Takano, M. Zako, T. Okazaki, K. Terada, Terada microstructure-based evaluation of the influence of woven architecture on permeability by asymptotic homogenisation theory, *Composites Science and Technology* 62 (2002) 1347–1356.
- 6 F. Robitaille, A. Long, M. Sherburn, C. Wong, C. Rudd, Predictive modelling of processing and performance properties of textile composite unit cells: current status and perspectives, in: *Proceedings ECCM-11, 2004*, cd-edition.
- 7 E. Belov, S. Lomov, I. Verpoest, T. Peeters, D. Roose, Modelling of permeability of textile reinforcements: lattice boltzmann method, *Composites Science and Technology* 64 (2004) 1069–1080.
- 8 C. Wong, A. Long, M. Sherburn, F. Robitaille, P. Harrison, C. Rudd, Comparisons of novel and efficient approaches for permeability prediction based on the fabric architecture, *Composites Part A* 37 (6) (2006) 847–857.
- 9 J. Delerue, S. Lomov, R. Parnas, I. Verpoest, M. Wevers, Pore network modelling of permeability for textile reinforcements, *Polymer Composites* 24 (3) (2003) 344–357.
- 10 C. V. Sienlen, Walker diffusion method for calculation of transport properties of finite composite systems, *Physical Review E* 65 (2002) 1–6.
- 11 I. Verpoest, S. Lomov, Virtual textile composites software wisetex: integration with micro-mechanical, permeability and structural analysis, *Composites Science and Technology* 65 (15-16) (2005) 2563–2574.
- 12 B. Verleye, M. Klitz, R. Croce, D. Roose, S. Lomov, I. Verpoest, Computation of permeability of textile with experimental validation for monofilament and non crimp fabrics, *Computational Textiles*, Vol. 55, Springer, 2007, pp. 93–110.
- 13 H. Brinkman, On the permeability of media consisting of closely packed porous particles, *Applied Scientific Research* 1 (1).
- 14 M. Griebel, T. Dornseifer, T. Neunhoffer, *Numerical Simulation in Fluid Dynamics, a Practical Introduction*, SIAM, Philadelphia, 1998.
- 15 <http://wissrech.iam.uni-bonn.de/research/projects/NaSt3DGP>
- 16 G. Morren, J. Gu, H. Sol, B. Verleye, S. Lomov, Permeability identification of a reference specimen using an inverse method, in: *SEM Annual Conference and Exposition, 2007*, pp. 1–8, cd-edition.
- 17 M. Nordlund, T. S. Lundström, Numerical study of the local permeability of noncrimp fabrics, *Journal of Composite Materials* 39 (10) (2005) 929–947.
- 18 S. Lomov, I. Verpoest, T. Peeters, D. Roose, M. Zako, Nesting in textile laminates: geometrical modelling of the laminate, *Composites Science and Technology* 63 (7) (2002) 993–1007.
- 19 S. Lomov, I. Verpoest, Model of shear of woven fabric and parametric description of shear resistance of glass woven reinforcements, *Composites Science and Technology* 66 (7-8) (2006) 919–933.
- 20 C. Lai, W. Young, Model resin permeation of fiber reinforcements after shear deformation, *Polymer Composites* 18 (5) (1997) 642–648.